ELSEVIER

Journal of Structural Geology 28 (2006) 83–98

JOURNAL OF STRUCTURAL GEOLOGY

www.elsevier.com/locate/jsg

Geological and mathematical framework for failure modes in granular rock

Atilla Aydin[a,*], Ronaldo I. Borja[b], Peter Eichhubl[a,1]

[a]*Department of Geological and Environmental Sciences, Stanford University, Stanford, CA 94305, USA*
[b]*Department of Civil and Environmental Engineering, Stanford University, Stanford, CA 94305, USA*

Received 3 November 2004; received in revised form 19 July 2005; accepted 28 July 2005
Available online 18 October 2005

Abstract

We synthesize all the available data on failure processes in granular rock and provide a geological framework for the corresponding structures. We describe two categories: (1) sharp discontinuities made up of two surfaces similar to elastic crack models, and (2) tabular structures resulting from strain localization into narrow bands. Each of these categories includes types predominated by shear and/or volumetric deformation. While shear failure can be in two different modes as sliding and tearing, the volumetric failure has two diametrically opposite types: compaction (contraction) and dilation (extension). Thus, we distinguish among bands predominantly by shearing, shortening, and extension. Slip surfaces, pressure solution surfaces, and joints represent corresponding sharp discontinuities. A survey of observations and measurements from naturally occurring structures indicates that although isochoric shear and pure volumetric deformation types represent end members, a complete spectrum of combined shear and volumetric deformation occurs in nature. Field observations also show that sharp structures overlap older narrow tabular structures in the same rock. This switch in failure modes is attributed to changing rock rheology and/or loading conditions.

In the mathematical modeling, we focus on the strain localization into narrow tabular bands using classical bifurcation theory combined with nonlinear continuum mechanics and plasticity. We formulate a family of three invariant plasticity models with a compression cap and capture the entire spectrum of failure of geomaterials. In addition, we draw an analogy between the concepts of 'strong' and 'sharp' discontinuity and classic elastic crack representations to complement the mathematical treatment of the failure modes.

Keywords: Failure modes; Deformation bands; Shear bands; Compaction bands; Dilation bands; Fracturing of sandstone

1. Introduction

Failure of soil, sand, and granular rock under natural and laboratory loading conditions involves a variety of micromechanical processes (Wong et al., 1997) that produce several geometrically, kinematically, and texturally distinct types of natural structures (Davatzes and Aydin, 2004). This paper provides a geological and mathematical framework for these failure processes and their structural products. The simplest of common structures is made up two subparallel surfaces. Joints, for example, fall into this category (Pollard and Aydin, 1988). Shear fractures or faults are often idealized by relative sliding of two surfaces in frictional contact (Jaeger and Cook, 1979) and are represented by elastic crack models (Pollard and Segall, 1987). Another category of structures resulting from failure in porous granular rock is a narrow tabular zone of localized strain (Friedman and Logan, 1973; Engelder, 1974) referred to as a deformation band (Aydin, 1978). The most common mode in this category is shear bands characterized predominantly by shearing with either minor compaction or minor dilation (Antonellini et al., 1994a). Shearing with no or very little volume change (isochoric or simple shear), and pure compaction/dilation with no macroscopic shearing also exist and represent the basic end members. Deformation bands with predominantly volume change have been reported from field studies (Hill, 1989; Antonellini et al.,

* Corresponding author.
E-mail address: aydin@pangea.stanford.edu (A. Aydin).
[1] Present address: Department of Physical and Life Sciences, Texas A&M University-Corpus Christi, Corpus Christi, TX 78412, USA.

0191-8141/$ - see front matter © 2005 Elsevier Ltd. All rights reserved.
doi:10.1016/j.jsg.2005.07.008

1994a; Çakir and Aydin, 1994; Mollema and Antonellini, 1996; Sternlof and Pollard, 2001; Du Bernard et al., 2002). Some of these localization phenomena were successfully simulated in the laboratory (Dunn et al., 1973; Olsson, 1999; Mair et al., 2000; Haimson, 2001; Wong et al., 2001) and were modeled theoretically (Rudnicki and Rice, 1975; Aydin and Johnson, 1983; Issen and Rudnicki, 2000; Bésuelle and Rudnicki, 2004; Borja and Aydin, 2004).

The first part of this paper synthesizes the available information in the literature and provides a geological framework for the entire spectrum of failure modes and related structures in granular rock. The second part provides a brief geomechanical framework for these features for the purpose of introducing a theoretical foundation for the range of the structures described earlier.

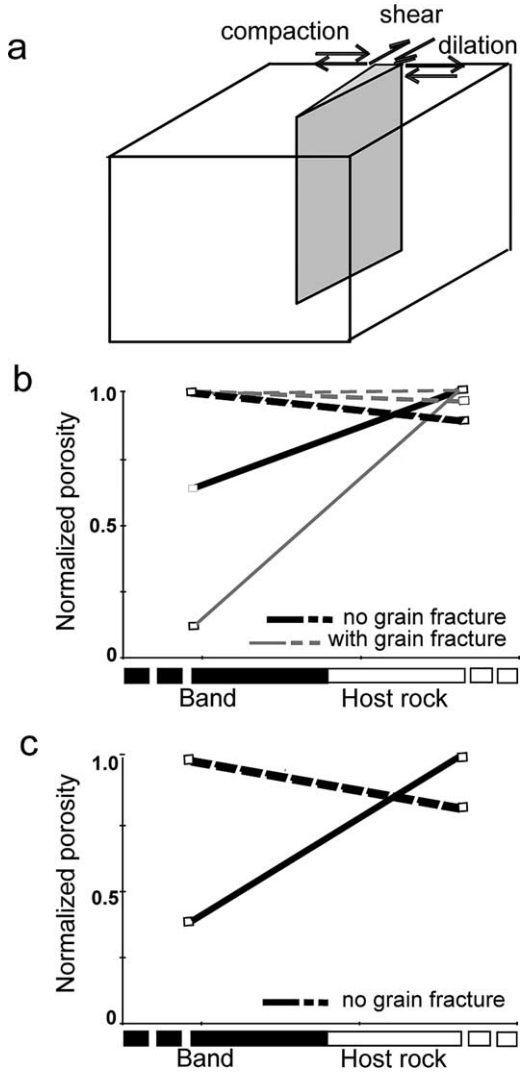

Fig. 1. (a) Idealized shear, compaction, and dilation modes. (b) Trends for volume change within shear bands with respect to the parent rock. From Aydin (1978), Antonellini and Aydin (1994) and Antonellini et al. (1994a). (c) Trends for volume change within compaction and dilation bands. Based on unpublished data of Antonellini, Aydin, Pollard, and D'Onfro and data from Mollema and Antonellini (1996) and Du Bernard et al. (2002).

2. Classification of failure structures in sandstone

We propose a broad classification of failure modes in granular rock, which includes two major categories and several subdivisions (Fig. 1a):

(1) Deformation bands
  (1.1) Shear deformation bands
    (1.1.1) Isochoric shear bands
    (1.1.2) Compactive shear bands
    (1.1.3) Dilatant shear bands
  (1.2) Volumetric deformation bands
    (1.2.1) Compaction bands
    (1.2.2) Dilation bands
(2) Sharp discontinuities
  (2.1) Fractures with predominantly shearing/slip surfaces
  (2.2) Discontinuities with predominantly volumetric deformation
    (2.2.1) Joints (dilatant/opening fractures)
    (2.2.2) Pressure solution surfaces (compaction/closing fractures)

The first category in (1) encompasses structures that form by localization of strain into narrow tabular bands. These narrow zones of shearing and volumetric deformation are called deformation bands (Aydin, 1978) following the use of the term in the engineering literature for localized failure zones (Argon, 1975; Rudnicki and Rice, 1975). The same structures are sometimes called Lüders' bands (Friedman and Logan, 1973; Olsson, 2000) or granulation seams (Pittman, 1981). We here consider two types of deformation bands (Fig. 1a) based on their kinematic attributes: (1) bands predominated by shearing, referred to as shear bands in this paper for simplicity (Figs. 1a and b and 2a), and (2) bands predominated by volumetric deformation (Fig. 1a and c). The latter group can be subdivided into compaction bands that are characterized by a volume decrease with respect to the undeformed parent rock and dilation bands that are characterized by a volume increase (Fig. 1c). Shear bands may have either dilatant or compactive volumetric deformation. Without being specific on the relative magnitudes of shear and volumetric components within a band, we rely on the presence of a noticeable shear displacement gradient across the band for identification of shear bands.

Sharp discontinuities are initially made up of two surfaces that move either parallel or perpendicular to the surfaces. If the movement of the two surfaces is perpendicular to each other, it may be either away from, or toward, each other (opening or mode-I and closing or anti-crack, respectively). If the movement of the surfaces is parallel to each other, the products are the same as the idealized concept of shear fractures (Pollard and Segall, 1987) that grow in-plane either in sliding

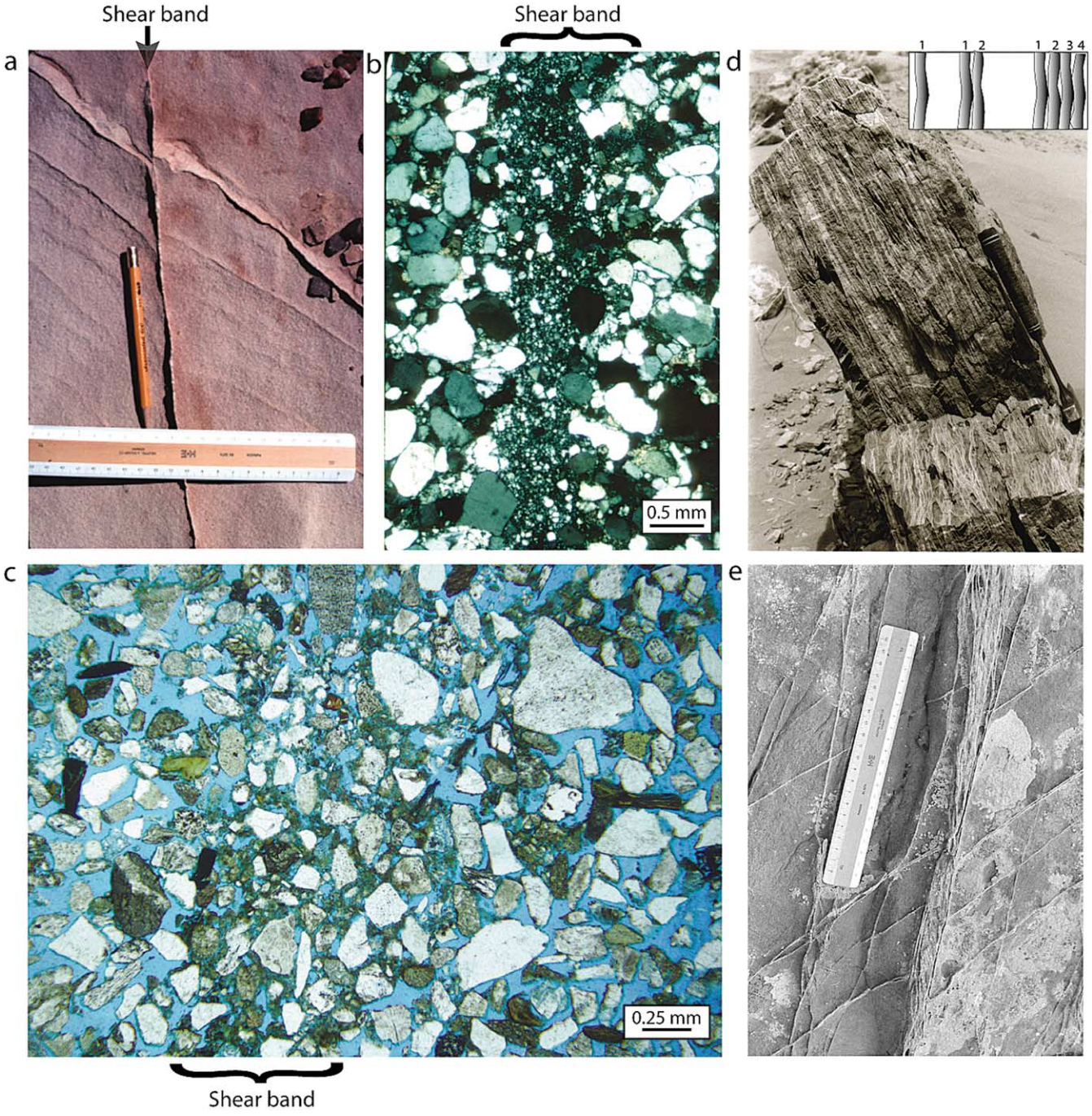

Fig. 2. (a) Outcrop photo showing a shear band (arrow) in Entrada sandstone, San Rafael Desert, Utah. The band shows a few mm left lateral slip. (b) Thin section image of a shear band (arrow) marked by a smaller grain size (i.e. cataclasis) in the Entrada Sandstone in San Rafael Desert. (c) A shear band without cataclasis in unconsolidated sediments, McKinleyville, northern California. (d) Outcrop photo of a zone of shear bands in Entrada sandstone, San Rafael Desert, Utah. Inset shows schematically lateral widening of a deformation band zone. Note hammer for scale. (e) Outcrop photo of a network of shear bands and zones of shear bands in San Rafael Desert, Utah.

mode (mode-II) or tearing mode (mode-III). Out of plane growth in any combination of one of these modes with opening or closing (mixed modes) is also possible. Thus, sharp discontinuities are initially similar to the elastic crack concepts with the caveat that progressive sliding will eventually produce accompanying deformation adjacent to the sliding surfaces.

3. Micromechanics of failure in deformation bands

The nature of deformation within individual bands is controlled by textural properties of the parent rock. Typical granular rocks are made up of grains, pores, and cement. Deformation of these rocks involves change in shape and size of one or more of these constitutive elements (Fig. 3).

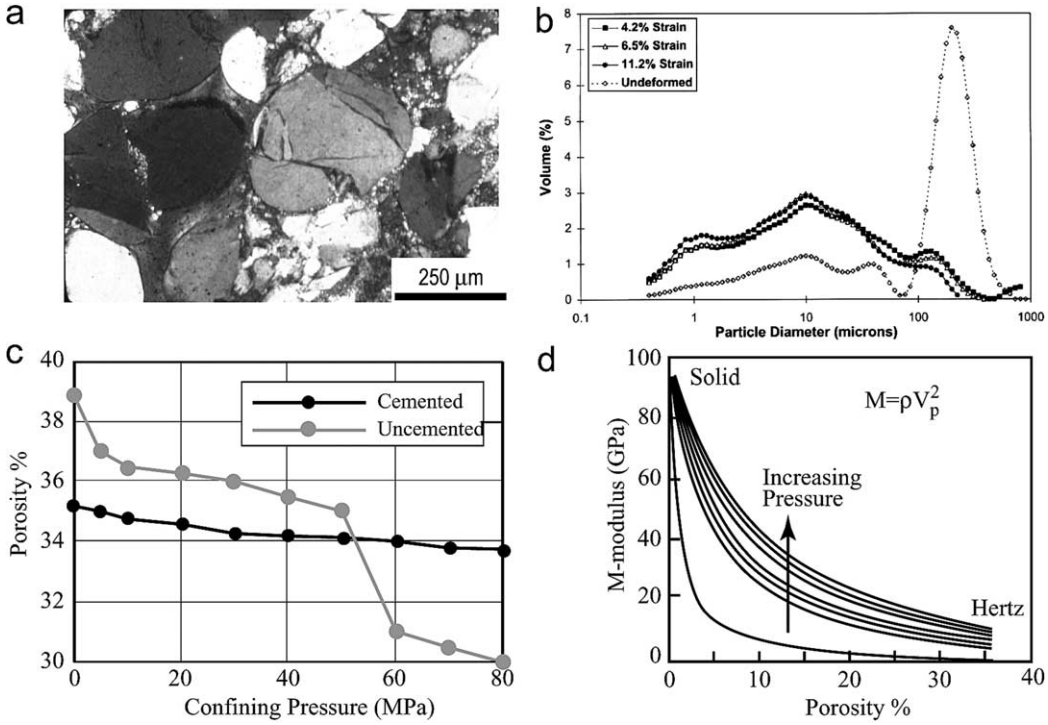

Fig. 3. (a) Image of initial grain fractures in sandstone. (b) Grain size distribution in shear bands with varying amounts of strain compared with undeformed sandstone. From Mair et al. (2000). (c) Plots showing the relationship between porosity and confining pressure for cemented and non-cemented granular material. From Dvorkin and Nur (1996). (d) Dependence of M-modulus (the bulk density of aggregate times the square of P-wave velocity) on porosity for various effective pressures. From Dvorkin and Nur (1996).

Among these three elements, grains form the skeleton of a granular rock. The strength of this skeleton depends on the strength of constituting grains and the nature of cement supporting the grains. Grain mineral composition plays an important role in failure processes due to differences in shape, strength, susceptibility to cleavage fracture, and chemical stability. Grains deform in three basic modes: (1) translation and rotation, (2) dissolution, and (3) internal strain dominated by fracturing in brittle states. Relative displacement and rotation of intact grains and fracturing of grains in porous sandstone are primarily controlled by the Hertzian grain-to-grain interaction (Gallagher, 1987; Zhang et al., 1990). Dissolution is generally dependent on the overburden thickness or the burial depth (Bjørlykke and Høeg, 1997). If the stresses at grain contacts exceed the tensile strength of the grains or the fracture toughness in general, they break, leading to fragmentation and comminution (Fig. 3a and b), which are elements associated with cataclastic deformation. Pores impact volumetric deformation and control the strength of rock. They act as flaws and concentrate stresses that may lead to eventual failure by pore growth and coalescence (Berg, 1970, 1972; Antonellini et al., 1994a; Du Bernard et al., 2002) or pore collapse (Aydin, 1978; Curran and Corrall, 1979). In addition, pores store fluids and thus facilitate transmission of forces to the skeleton in high fluid pressure environments. It has been well known, based on the effective stress law, that rocks under a high pore fluid pressure are considerably weaker (Hubbert and Rubey, 1959).

Following the principles summarized in the paragraph above, intergrain sliding (grain translation and rotation), grain fracturing, pore volume change, and pressure solution appear to be the fundamental micromechanical processes that characterize the failure modes and their structural products in granular rocks under upper crustal conditions. Grain fractures (Fig. 3a) leading to grain size reduction (Fig. 3b) and changes in pore volume by either pore collapse or diagenetic processes (Figs. 1a–c and 3c) are the two quantities that can readily be identified and measured. However, intergrain movements are very difficult to detect in granular rock because of the lack of pre-existing markers.

All micromechanical processes are greatly influenced by diagenetic reactions that affected the host rock prior to deformation (Groshong, 1988; Bjørlykke and Høeg, 1997). Cementation and dissolution reactions control the amount, distribution, shape, and strength of cement and are therefore crucial in the failure processes in granular rocks. Cement exerts resistance to intergranular movement and distributes contact forces thereby reducing the stress concentration leading to grain breakage (Bernabé et al., 1992; Dvorkin and Nur, 1996; Shah and Wong, 1997; Wilson et al., 2003). With increasing burial depth and cementation, the deformation behavior of granular materials thus changes. General trends lead from localized tabular modes of elastic/plastic

deformation to dilatant and sharp modes of elastic deformation with increasing mechanical compaction and diagenetic porosity reduction. These trends correspond to the change from a contact-based Hertzian constitutive behavior to that of a solid framework with decreasing porosity as expressed in a gradual increase in M-modulus (Fig. 3d) (Dvorkin and Nur, 1996). M-modulus is ρV_p^2, where ρ is the bulk density of the aggregate and V_p is the P-wave velocity.

These general depth trends could potentially be reversed due to dissolution of framework minerals and of earlier pore cement leading to the creation of secondary porosity that may again bring up pore controlled stress concentrations and may allow compactive modes of deformation localization at depth.

4. Shear bands

The diagnostic feature of shear bands is a macroscopic shear offset across a tabular zone of finite small width with respect to the other two dimensions (Fig. 2a). Shear offset can be determined by previously continuous markers such as beds or older shear bands. Shear bands in granular rocks have limited offsets on the order of a few millimeters to centimeters (Engelder, 1974; Antonellini et al., 1994a; Fossen and Hesthammer, 1997). The average shear strain calculated from these quantities is on the order of unity (Aydin, 1978). The length dimension of single shear bands is also limited to less than 100 m (Fossen and Hesthammer, 1997). Therefore, it is necessary to form new shear bands in order to widen (or lengthen) a shear band structure in a manner schematically illustrated by the inset in Fig. 2d (Aydin and Johnson, 1978). This process leads to the formation of a zone of shear bands, which is composed of a number of closely spaced, subparallel distinct shear bands (Fig. 2d). Well-developed shear zones such as those in Fig. 2d are associated with a slip surface that accommodates a large magnitude of slip and marks the appearance of a sharp discontinuity along usually one side of a zone of shear bands. Each of these elements may occur in a network composed of two or more sets (Fig. 2e). Shear bands and shear band zones are typically more resistant to weathering thus forming spectacular geomorphic features in the field (Aydin and Johnson, 1978; Davis, 1999).

A thin section view of a shear band (Fig. 2b and c) shows evidence for micromechanical processes responsible for its formation. Grain fracturing (Fig. 3a) can be detected in initial stages where the grains are damaged but not yet demolished. In more advanced stages of deformation, grain fracturing and grain crushing are reflected by grain size reduction or comminution (Fig. 3b) and change of grain shape within the localized zone of deformation. Typically, intense deformation results in broadening of the grain size distribution within shear bands (Aydin, 1978; Menéndez et al., 1996; Mair et al., 2000; DiGiovanni et al., in press) due to increase in the number of smaller grains (Fig. 3b). These processes as well as other textural and diagenetic changes are usually referred to as 'cataclasis' (Borg et al., 1960). Although shear bands are commonly associated with grain fracturing and grain size reduction, these processes are not prerequisites for every shear band formation. For example, Fig. 2c shows a shear band in unconsolidated soft sediments initially studied by Cashman and Cashman (2000). The band has noticeable shear offset in outcrop. There is microscopic and macroscopic evidence for rotation, translation, and differentiation of grains but very little grain fracturing is evident in thin section photomicrographs. From a theoretical point of view, it is possible to move grains with respect to each other without grain fracturing (Dvorkin and Nur, 1996; Borja et al., 2000; Wong et al., 2004). This mode of deformation is referred to as particulate flow (Borradaile, 1981; Rawling and Goodwin, 2003).

Although rare, shear bands without any significant volumetric component of deformation also occur judging from the same range of porosity values for some shear bands and the corresponding parent rocks within the accuracy of the measurements (Antonellini et al., 1994a; see top flat line in Fig. 1b). This type of shear bands will be referred to as 'isochoric' shear bands representing the type of deformation known as 'simple shear' in geology. Most shear bands, however, undergo volumetric deformation in addition to shearing (Aydin, 1978; Antonellini and Aydin, 1994; Antonellini et al., 1994a,b; Bésuelle, 2001). These mixed mode bands, regardless of the relative magnitude of shear and volumetric components of deformation, are referred to as 'compactive shear bands' or 'dilatant shear bands'. Compactive and dilatant shear bands are characterized predominantly by shearing but are also associated with volume decrease or increase, respectively (Fig. 1b). It is, therefore, essential to characterize the volume change within tabular shear bands. Several methods were employed to determine pore or skeleton volume and porosity within bands and in relatively pristine rocks nearby. These methods include liquid/helium porosimetry or immersion of samples into a liquid with proper pre- and post-immersion measurements, petrographic image analysis (Antonellini et al., 1994a), X-ray computerized tomography (Antonellini et al., 1994b), and traditional point counting using a petrographic microscope or secondary or backscatter electron images. The formation of cement after deformation makes point counting and the determination of the skeleton or minus-cement porosity the preferred method of quantifying porosity changes associated with deformation.

5. Volumetric deformation bands

Deformation bands that lack evidence of macroscopic shear offset form predominantly by volumetric deformation and are therefore called volumetric deformation bands. Volume change in bands with respect to the undeformed

state may be either positive or negative and is expressed by porosity increase (dilation) or decrease (compaction), respectively (Figs. 4 and 5).

5.1. Compaction bands

Compaction bands in Aztec sandstone of Valley of Fire State Park in southeastern Nevada were the earliest examples for compaction localization reported in the literature (Hill, 1989; Çakir and Aydin, 1994). Following these initial discoveries, similar structures were recognized in Navajo sandstone (Mollema and Antonellini, 1996), an equivalent stratigraphic unit exposed in Kaibab Monocline near the Utah–Arizona border. Fig. 4 shows a single compaction band (a), a network of compaction bands made up of two distinct sets (b), an example of a zone of compaction bands (c), and X-ray computerized tomographic image (CT) for porosity inverted from the corresponding density distribution from the sample in Fig. 4c. Examination of compaction bands in outcrops shows no detectable shear offset and a somewhat thicker band compared with the average thickness of shear bands at the same locality (Antonellini and Aydin, 1994; Çakir and Aydin, 1994). The porosity measurements indicate a porosity decrease from about 20% to about 5% or less (Fig. 4d). Sternlof and Pollard (2001, 2002) measured thickness changes along individual compaction bands in Aztec sandstone in Valley of Fire location and calculated corresponding displacement

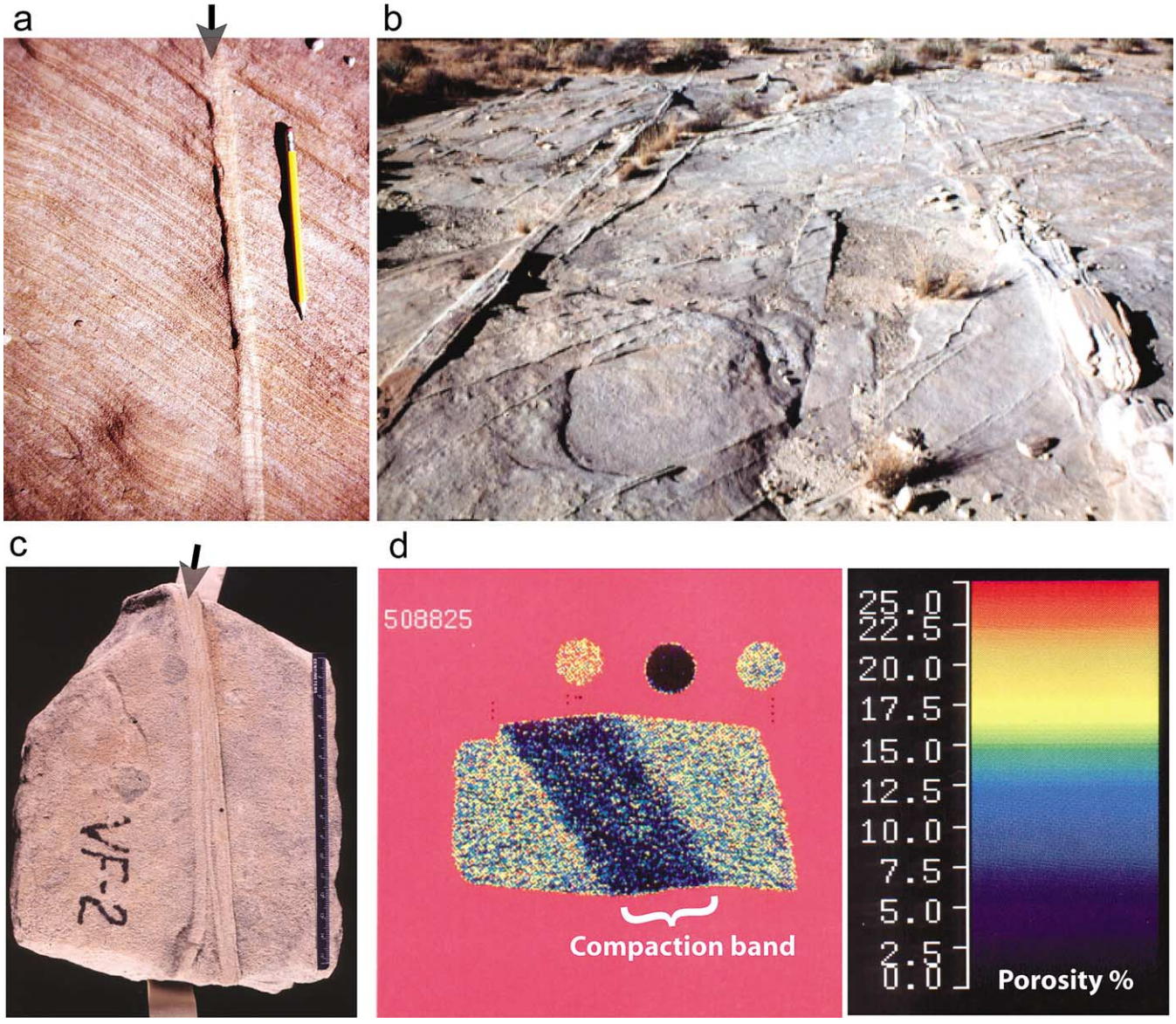

Fig. 4. Compaction bands in Aztec sandstone at Valley of Fire, Nevada. (a) Outcrop photo of a compaction band showing positive relief relative to the surrounding undeformed sandstone. No macroscopic shear across the band is detectable. (b) A photograph showing a network of compaction bands at the same locality. (c) Photograph of a sample with compaction bands. Scale on right in inches. (d) CT scan of the sample in (c) showing porosity distribution inverted from density distribution. The average porosity of the parent sandstone is about 20%, whereas the porosity of the band is about 5–7%.

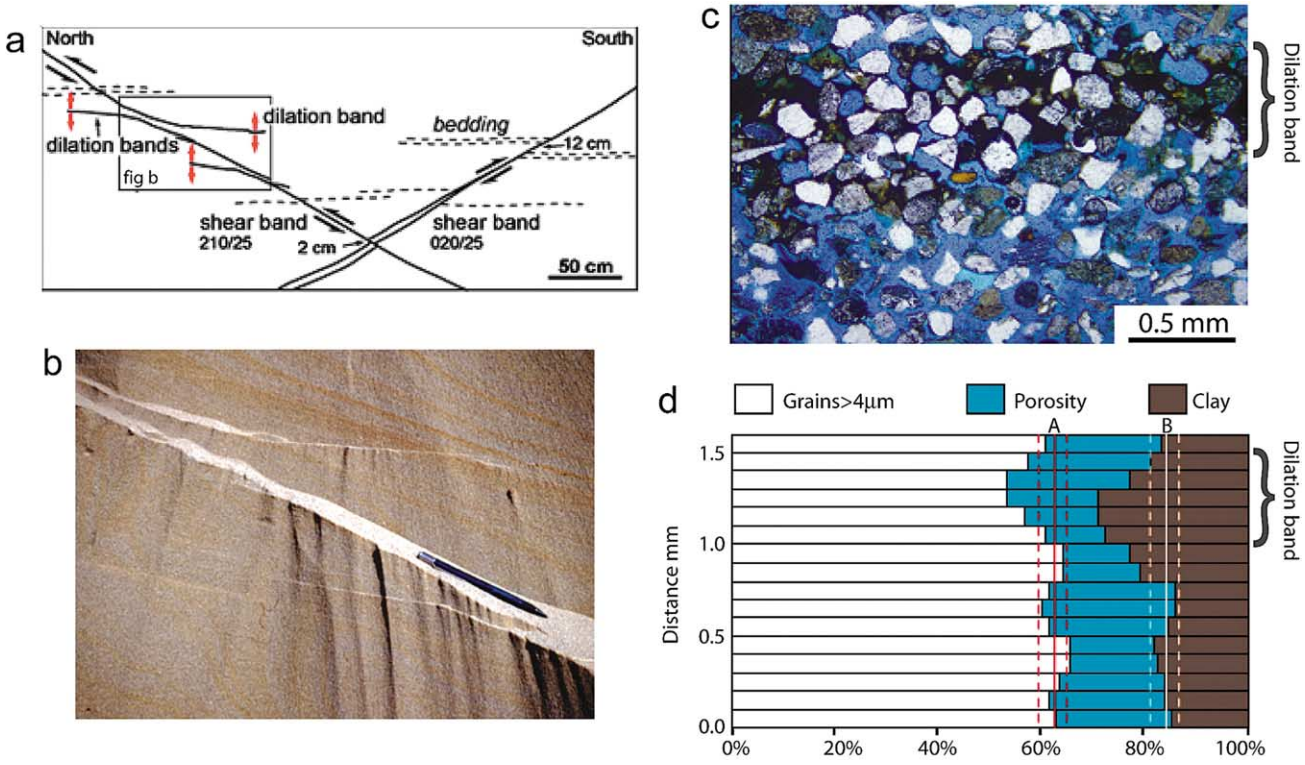

Fig. 5. Dilation bands in unconsolidated sand near McKinleyville, northern California. (a) Mapping showing outcrop pattern of bands comprising two sets of shear bands (inclined) and one set of dilation bands (nearly horizontal). (b) Detailed photograph (see location in (a)) showing one set of shear bands and one set of dilation bands connected to the ends of the shear bands segments. (c) Thin section image of a portion of the dilation band. Note that pores within the band are filled by clay minerals (dark). (d) Porosity distribution across the thin section determined by point counting. The graph shows a 7% (±3%) increase in skeleton or minus-cement porosity ('A') within the band.

discontinuities based on average porosity of the bands. They suggested that the compaction bands have a form similar to that predicted from an anti-crack under elastic loading using linear elastic fracture mechanics. They also proposed that the in-plane growth and propagation of these structures are similar to that of opening mode cracks.

5.2. Dilation bands

Deformation bands with porosity increase with respect to the undeformed state and no macroscopic shear offset have been reported by Du Bernard et al. (2002). In this case, the lack of a shear offset was determined based on crosscutting relations of deformation bands with depositional markers and with other deformation bands that had formed earlier. Fig. 5 shows an outcrop pattern of dilation bands associated with shear bands (a), a detailed photograph of the area marked by a square in the map (b), a thin section image of a dilation band (c), and porosity distribution through a thin section image including one of the dilation bands as determined by point counting (d). Dilation bands bisect two apparently conjugate sets of shear bands with thrust offset and are connected to the ends of the segments of the shear bands. This configuration indicates that the dilation bands were subjected to the maximum tangential tensile stresses as inferred from the sense of the offset on the shear structure and the idealized elastic stress state at its tip region (Fig. 5a,c). Pore space within portions of the band is filled by dark clay minerals and organic matter (Fig. 5c), interpreted as the result of particulate infiltration by moving ground water. This infilling material likely prevented collapse of the locally increased pore space after loading had ceased. In order to determine the porosity during the time of the deformation, the skeleton or minus cement porosity was calculated (Du Bernard et al., 2002). The graph in Fig. 5d shows approximately 7% (±3%) porosity increase within the band.

6. Sharp discontinuities in granular rock

Perhaps some of the most ubiquitous planar discontinuities in rocks including granular rocks are joints (Fig. 6a). Joints are characterized by opening mode displacement discontinuity normal to the two surfaces that define them. The surfaces commonly display well-known morphology often referred to as plumose structure with linear hackle and concentric rib marks (Fig. 6b). Joints in layered granular rock commonly are perpendicular to the layers (Fig. 6a and b) in which they occur. In both map view and vertical sections joints are short and typically have many segments. For brevity, we refer to the review paper by Pollard and Aydin (1988) on

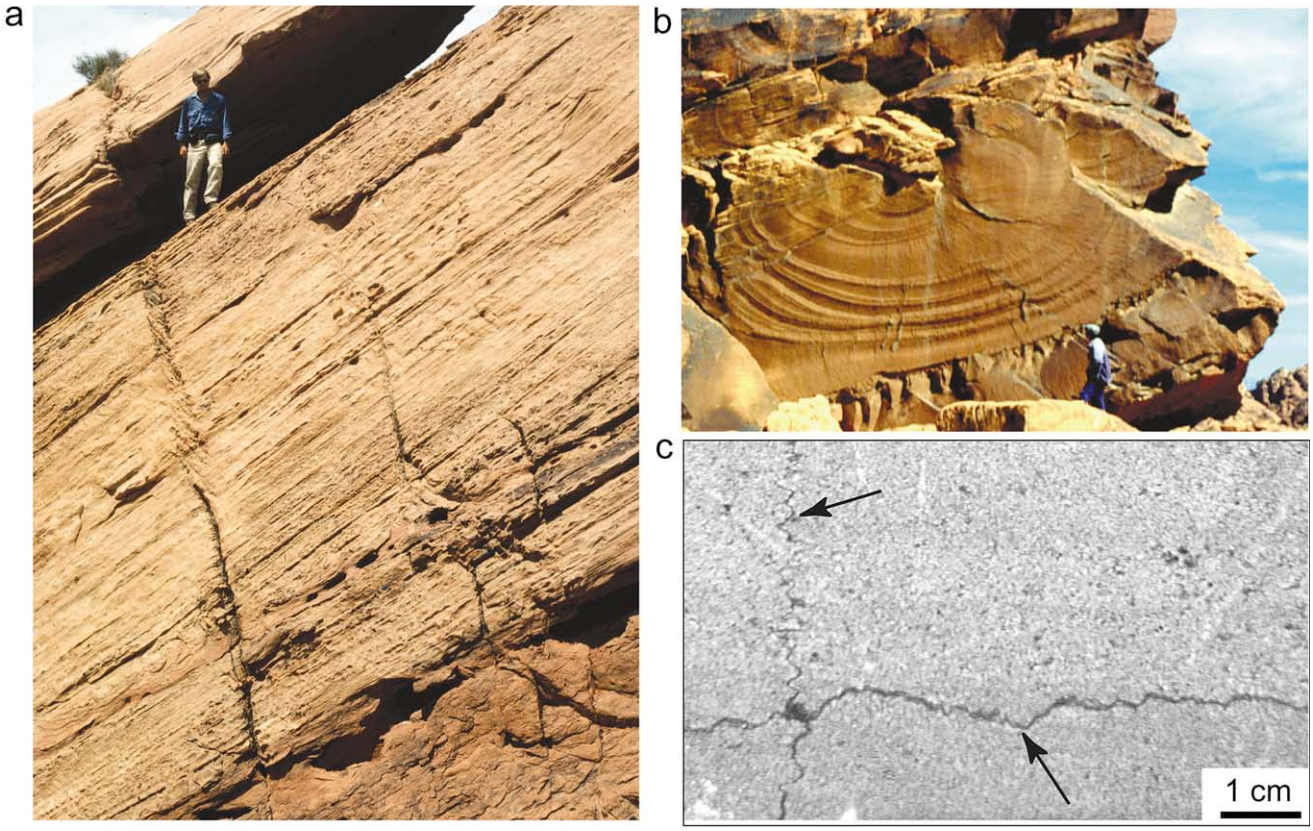

Fig. 6. Outcrop photos of sharp discontinuities accommodating volumetric strain. (a) A set of joints in sandstone. Person for scale. (b) A joint surface with hackles and rib marks. Person on lower right for scale. Both (a) and (b) from Aztec sandstone, Valley of Fire, Nevada. (c) Thin section photomicrograph of orthogonal bedding-parallel (horizontal) and bedding-perpendicular (vertical) solution surfaces (arrows) in sandstone. Core sample from 4800 m depth, the North Sea.

the broad subject of jointing in granular rock and the characteristics of joints.

Planar closing structures or anti-cracks (Fletcher and Pollard, 1981) are associated with mineral dissolution at grain-to-grain contacts and removal of the dissolved material by diffusive or advective mass transfer (Al-Shaieb et al., 1994; Renard et al., 2000). Fig. 6c shows an excellent example for this type of structure in a sandstone core from a depth of 4800 m from the North Sea. Note that the flat solution structure is bed-parallel whereas the orthogonal one is bed-perpendicular and is believed to be tectonic in origin.

Planar structures composed of two surfaces in contact and subjected to shearing are idealized as shear fractures/faults (Pollard and Segall, 1987) and are envisioned to occur in granular rock. In these structures, movement of the surfaces is predominantly parallel to each other. The structural products are the same as those formed by the idealized concept of shear fractures propagating in-plane either in mode II or mode III or out-of-plane in mixed modes. Another structure that is similar to the idealized shear fracture is slip across a pre-existing planar weakness. However, these structures differ from the idealized shear fractures by their characteristic out of plane propagation as will be described in the following section.

As opposed to experimental studies performed on samples with limited size and therefore limited heterogeneity, natural deformation of sandstone is always influenced by pre-existing elements that may be weaker or stronger than the typical rock matrix. Pre-existing features weaker than the surrounding rock matrix are crucial for rock failure. Some prominent weaker pre-existing elements are depositional features indigenous to rock formation whereas some others are inherited from earlier deformation events. Bedding planes, for example, are weak planes of depositional origin and are ubiquitous in clastic sedimentary rocks. These planes are often the focus of slip concentration in flexed beds (Cooke et al., 2000). Structural elements inherited from an earlier deformation commonly impact subsequent failure processes especially in older rocks with multiple phases of deformation. Among these structural elements are microfractures and joints that are prone to subsequent shear failure (Brace and Bombolakis, 1963; Segall and Pollard, 1983). Many examples of this phenomenon in various sandstones have been documented in the literature (Cruikshank and Aydin, 1994; Myers and Aydin, 2004). The initial fundamental mechanism appears to be slip along a weak plane (Fig. 7a) in response to new shearing stresses resolved along the plane. This phenomenon results in a well known structure

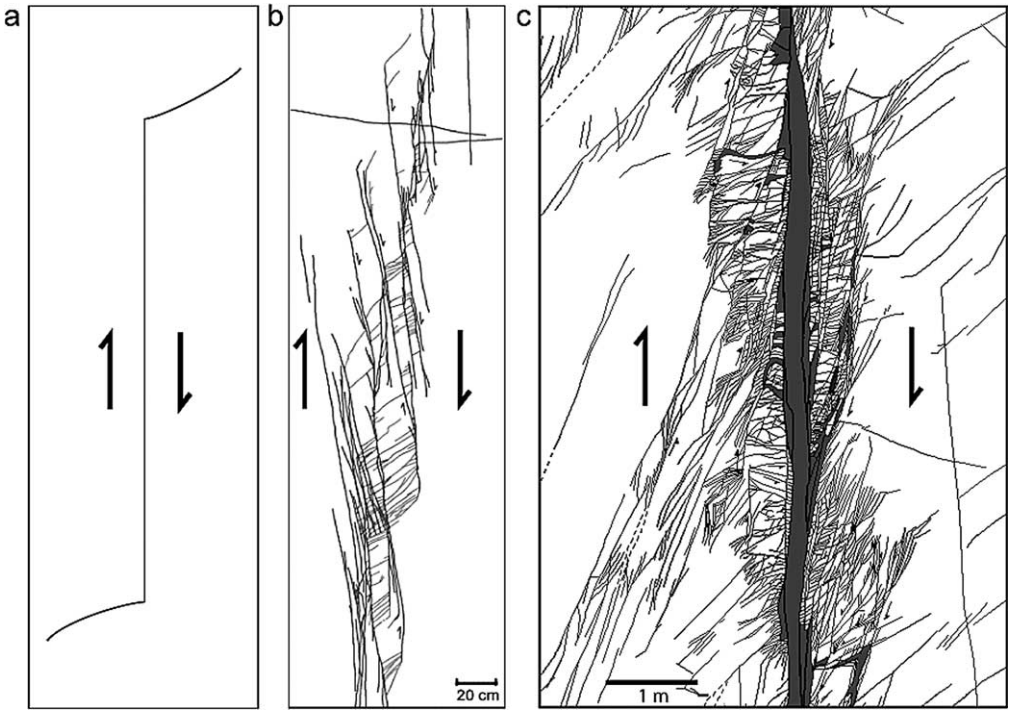

Fig. 7. Sketches depicting fault development by sliding along pre-existing planar weaknesses. (a) Conceptual model for shearing across a plane and formation of tail cracks. (b) Shearing across a series of en échelon joints forming pockets of highly damaged rock. (c) A fault zone (map view) with 14 m of right lateral slip. Notice fault rock (black) at the core and the surrounding damage zone made up of joints and sheared joints. (b) and (c) are from Myers (1999).

referred to as tail, splay, or kink crack (Cotterell and Rice, 1980; Engelder, 1987; Cruikshank et al., 1991). Fig. 7b illustrates shearing of a zone of joints and the associated splay joints formed at the tips of joints or at en échelon steps between neighboring joints (Myers and Aydin, 2004). Increased shearing across such a system produces a fault composed of a fault rock at the core and the surrounding damage zone (Fig. 7c).

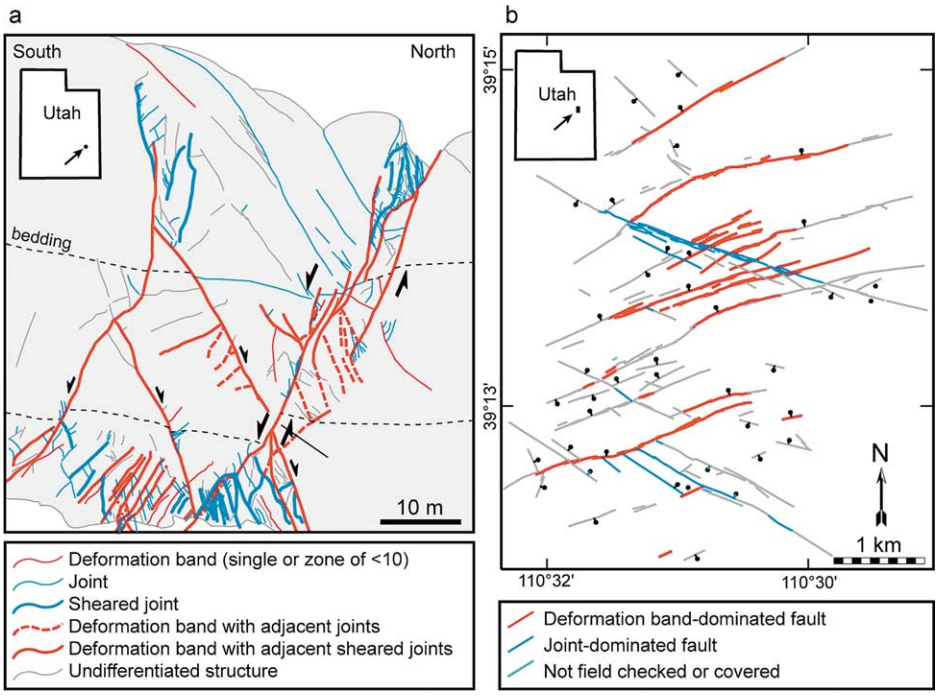

Fig. 8. Cross-section and map views that depict overprinting deformation mechanisms: (a) a subsidiary of the Moab fault in Entrada sandstone, Moab, Utah. Deformation bands (red) overprinted and cross-cut by joints (blue). Arrows mark slip sense. From Davatzes and Aydin (2003). (b) A system of four sets of normal faults in Navajo sandstone, Chimney Rock, San Rafael Swell, Utah. Bars indicate dip direction. From Davatzes et al. (2003).

Linear or spherical structures that are stronger than the surrounding rocks also focus subsequent deformation in their proximity. For example, shear bands and volumetric deformation bands in sandstone have been reported to localize subsequent jointing and sheared joint-based deformation (Zhao and Johnson, 1992; Çakir and Aydin, 1994; Davatzes et al., 2003; Davatzes and Aydin, 2004). Fig. 8a is a detailed map of a section of the Moab fault (Davatzes et al., 2003) and shows how joints and sheared joints overprint older shear bands, all of which have normal sense of slip. Fig. 8b summarizes the distribution of the failure modes along four sets of normal faults in the Chimney Rock area, northern San Rafael Swell, Utah (Davatzes and Aydin, 2004). This distribution suggests that some fault sets have different characteristics than other sets in the same locality in terms of failure structures reflecting sequential occurrence of failure modes along preferred orientations.

7. Mathematical capture of deformation bands

Deformation bands are often viewed as a result of an instability process when the constitutive relation for a material bifurcates from a smoothly varying deformation field into a highly localized deformation mode. Rudnicki and Rice (1975) proposed a stability analysis similar to that employed in Hill (1958), Thomas (1961) and Mandel (1966) solutions identifying the onset of a localization mode in dilatant frictional materials. Recently, Bésuelle and Rudnicki (2004) reviewed localization conditions for a broader spectrum of material behaviors.

In the small strain regime the general condition for the emergence of a deformation band in an elastoplastic material is given by the equation

$$\det(\boldsymbol{A}) = 0, \qquad A_{ij} = n_k c^{\mathrm{ep}}_{ikjl} n_l, \tag{1}$$

where $\boldsymbol{A}$ (with components A_{ij}) is the so-called elastoplastic acoustic tensor, c^{ep} (with components c^{ep}_{ikjl}) is the tangential elastoplastic constitutive tensor, and $\boldsymbol{n}$ (with components n_k or n_l) is the unit normal vector to the band. In the finite deformation regime two alternative descriptions may be used for the planar band, one reckoned with respect to the reference configuration and a second reckoned with respect to the current configuration (Borja, 2002).

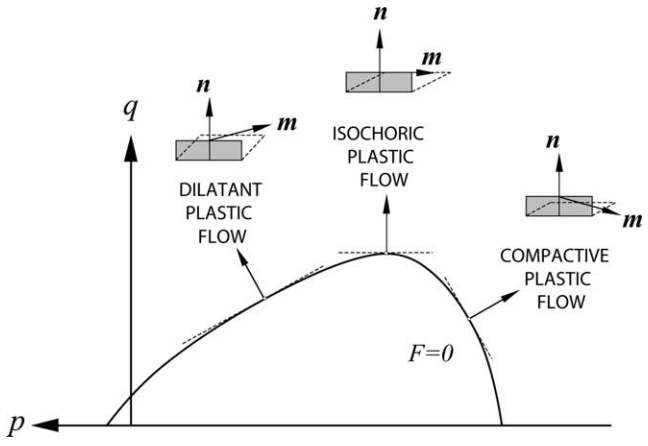

Fig. 9. Representation of dilatant shear band, simple shear band, and compactive shear band on *pq*-plane.

The above localization condition depends on the constitutive response of the material. For granular rocks, three-dimensional inelastic deformation is commonly described using theory of plasticity. The mathematical theory of plasticity assumes an additive decomposition of the total strain into elastic and plastic parts, and requires the specification of a yield surface defining the yield condition and a plastic potential function defining the direction of the plastic strain increment (Borja et al., 2003). The nature of the constitutive response is described through the tangential constitutive tensor c^{ep}.

To detect a possible bifurcation into a planar band the vanishing of the determinant of the acoustic tensor is checked at each stress state and for each possible band orientation. For simple constitutive models a closed form expression for the determinant condition is possible, but for other more complicated models a numerical search may be necessary to identify the critical band orientation $\boldsymbol{n}$ at which the vanishing of the determinant is satisfied for the first time. Apart from the critical band orientation, the eigenvalue problem implied in Eq. (1) also determines a (normalized) unit eigenvector $\boldsymbol{m}$ of the acoustic tensor $\boldsymbol{A}$ describing the instantaneous direction of the relative velocity jump of the two faces of the band, as shown pictorially in Fig. 9. The normalized eigenvector $\boldsymbol{m}$, which has not been fully exploited in the literature, is associated with the homogeneous equation

$$\boldsymbol{A}\cdot\boldsymbol{m} = \boldsymbol{0}, \tag{2}$$

and can be constructed for band orientation $\boldsymbol{n}$ at which the non-trivial Eq. (1) is first satisfied. Depending on the value of the resulting scalar product $\boldsymbol{m}\cdot\boldsymbol{n}$, we may have a simple shear band, a compactive or dilatant shear band, or a pure compaction or pure dilation band. The precise nature of the deformation band is characterized according to the relations:

$$\begin{aligned}
&\boldsymbol{m}\cdot\boldsymbol{n} = 1 && \text{pure dilation band;}\\
&0 < \boldsymbol{m}\cdot\boldsymbol{n} < 1 && \text{dilatant shear band;}\\
&\boldsymbol{m}\cdot\boldsymbol{n} = 0 && \text{simple (isochoric) shear band;}\\
&-1 < \boldsymbol{m}\cdot\boldsymbol{n} < 0 && \text{compactive shear band;}\\
&\boldsymbol{m}\cdot\boldsymbol{n} = -1 && \text{pure compaction band.}
\end{aligned} \tag{3}$$

We emphasize that the above definitions pertain only to the instantaneous response at the onset of localization; whether or not these types of behavior will persist beyond the bifurcation point depends largely on how the material inside the band responds to further loading.

In the context of theory of plasticity the constitutive model requires a yield function F describing the limit of

elastic response in stress space, and a plastic potential function Q defining the direction of the plastic strain increment. The location of the stress point on the yield function at bifurcation determines the expected type of deformation band to which the solution will bifurcate. In many cases this is best represented pictorially on the p–q plane, where p is the mean normal stress and q is the norm of the stress deviation tensor (the latter stress is sometimes referred to as the Mises stress). Fig. 9 shows the yield surface on such a p–q plane. Note that such representation on the p–q plane is meaningful only when the yield and plastic potential functions depend on the first and second invariants of the stress tensor only. For three-invariant models the yield surface may be represented more generally on meridian and deviatoric planes (Borja et al., 2003).

As noted in Fig. 9 the expected type of deformation band to which the solution will bifurcate depends on the location of the stress point on the yield surface at the moment of localization. For example, localization, taking place on the dilatant side of the yield surface is expected to produce a dilatant shear band, whereas localization on the compactive side is expected to produce a compactive shear band. Furthermore, a material yielding at a constant volume is expected to produce a simple shear band. The scenarios shown in Fig. 9 are general trends—the precise mathematical formulations and theoretical analyses for different possible failure modes are described more specifically in a paper by Borja and Aydin (2004).

The localization model presented above includes the two special cases of pure compaction and pure dilation bands. They occur when $\boldsymbol{m} = \pm \boldsymbol{n}$, characterized either by a volume decrease or a volume increase with respect to the parent rock. For this type of deformation band Eq. (1) still applies; however, because of the special relation between the unit vectors $\boldsymbol{m}$ and $\boldsymbol{n}$ the localization condition simplifies to a certain form. Issen and Rudnicki (2000) and Rudnicki (2002) concluded that for axisymmetric loading the condition for a compaction band corresponds to a vanishing tangent modulus for the stress–strain curve. However, this conclusion is limited to the very simple case of axisymmetric loading and does not apply to the general case of three-dimensional loading. In three-dimensional loading, there exist three (usually distinct) principal stresses that are generally rotated with respect to a reference coordinate frame. In such a general case the condition set forth by Issen and Rudnicki does not hold.

In a recent article, Borja and Aydin (2004) formulated a general localization condition for the emergence of pure compaction and pure dilation bands applicable to three-dimensional loading and rotated principal stress axes. The formulation involved decomposition of the elastoplastic constitutive operator into a material part reckoned with

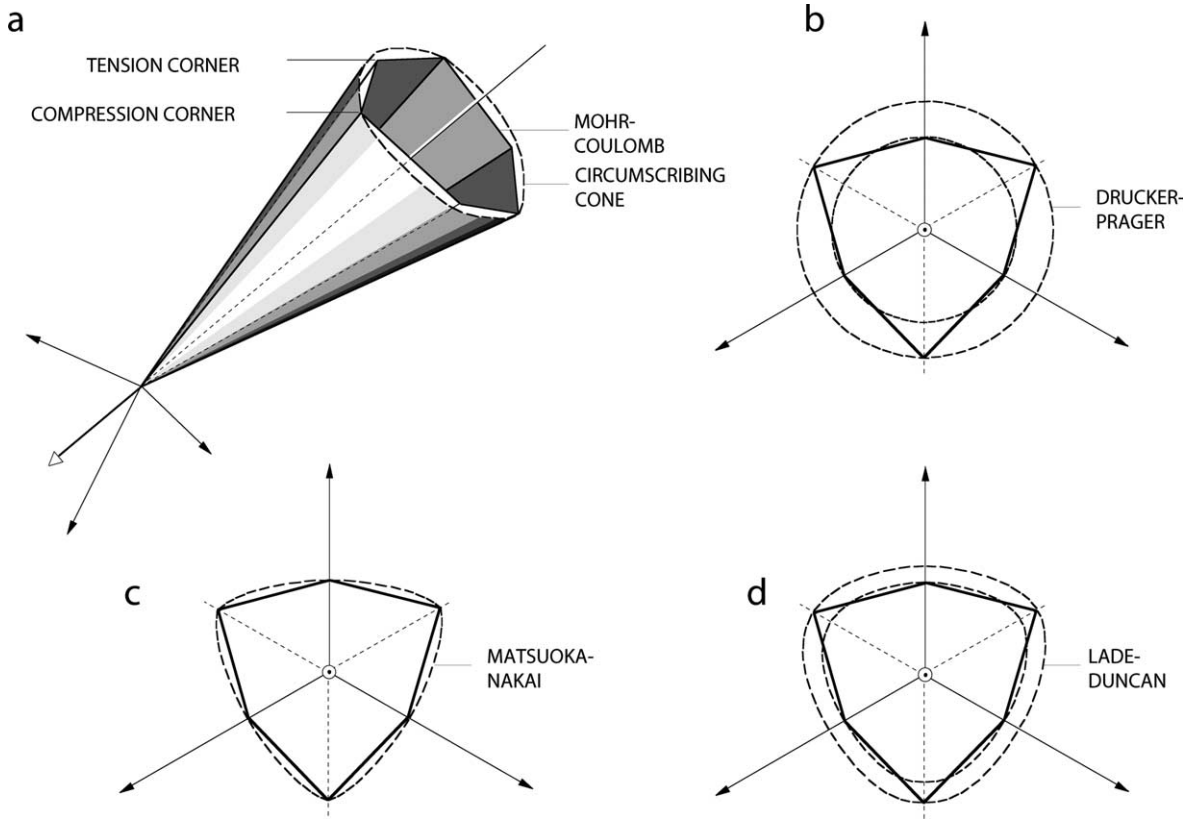

Fig. 10. Family of conical yield surfaces for dilatant frictional materials: (a) three-dimensional representation; (b)–(d) cross-sections on deviatoric plane for different plasticity models (after Borja et al., 2003).

respect to the principal stress axes, and a spin part reflecting the changing principal stress directions. For pure compaction/dilation bands Eq. (2) extracts only the material part in principal axes, and the localization condition reduces to the form:

$$a^{\mathrm{ep}}_{AA} = 0, \tag{4}$$

where a^{ep}_{AA} is the AA-(diagonal) component of the elastoplastic moduli matrix in principal axes (see Borja et al. (2003) for an elaboration of this elastoplastic moduli matrix). The precise nature of the volumetric deformation band formed, i.e. whether it is a pure compaction band or a pure dilation band, is determined by the requirement that the material inside the band continues to yield plastically at the moment of localization (Borja and Aydin, 2004). The above development is entirely new and represents a robust expression available for detecting, using bifurcation theory, the onset of a deformation band in an elastoplastic solid under general three-dimensional loading conditions.

Several elastoplastic constitutive models have been used in the past to describe yielding of granular rocks. The most familiar constitutive model that comes to mind is the Mohr–Coulomb plasticity model for dilatant frictional materials, where yielding depends on the major and minor principal stresses in compression but independent of the intermediate principal stress. In principal stress space the Mohr–Coulomb yield surface is represented by six planes forming a cone and having a cross-section of an irregular hexagon, as shown in Fig. 10a. The intersections of these planes form unwanted vertices that create enormous difficulties in the numerical implementation of the model. For this reason, smooth versions of the Mohr–Coulomb plasticity models have been developed in the past, including the Drucker and Prager (1952), Matsuoka and Nakai (1974), and Lade and Duncan (1975) plasticity models (Fig. 10b–d, respectively). There is ample evidence suggesting that some of these smooth versions describe the yield behavior of granular materials more accurately than does the Mohr–Coulomb plasticity model itself (Borja et al., 2003). As noted earlier, the selection of a constitutive model and calibration of the model parameters are crucial steps for an accurate prediction of the bifurcation point.

At higher confining pressures the material may exhibit plastic compactive behavior, and the cones of plastic yielding originally developed for dilatant frictional materials shown in Fig. 10 may not be appropriate anymore. In the present case we may need a yield function with a compression cap to capture plastic volumetric yielding, as well as a plastic potential function that also has a compression cap to enable the representation of the compactive plastic volumetric flow. Borja (2003) considers a family of two- and three-invariant teardrop-shaped yield functions shown in Fig. 11a–f, respectively, along with a family of plastic potential functions with similar shapes. These compression caps are essential for capturing the development of compactive shear bands.

The presence of the third invariant in the constitutive description implies that in the non-associative case the

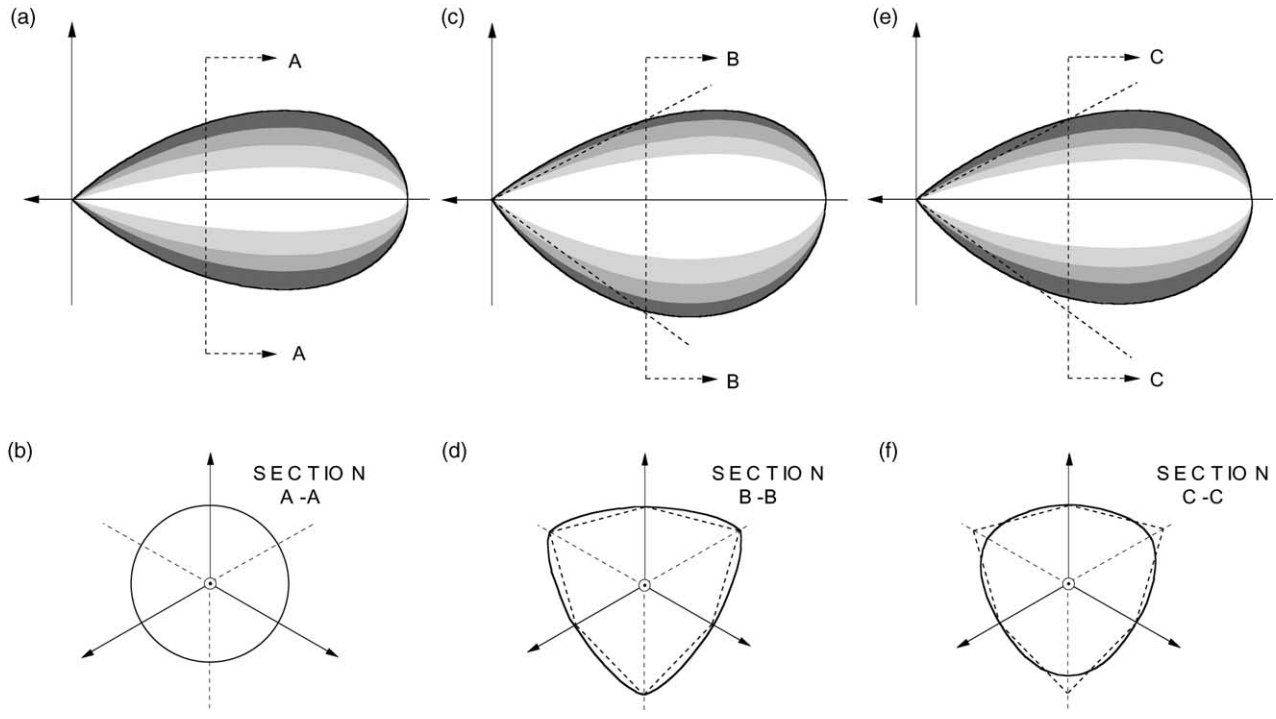

Fig. 11. Family of teardrop-shaped yield surfaces for frictional materials on meridian and deviatoric planes: (a) and (b) two-invariant yield surface; (c) and (d) capped Matsuoka–Nakai; (e) and (f) capped Lade–Duncan (after Borja, 2004).

plastic strain increment is not normal to the yield function on both the meridian and deviatoric planes. Two-invariant models such as the Drucker–Prager model can only capture non-associativity on the meridian plane; however, they preserve associative plasticity on the deviatoric plane even if the friction and dilation angles are not the same. This is because two-invariant functions always plot as circular regions on the deviatoric plane. Borja (2004) demonstrated that the presence of the third invariant in the constitutive description in fact enhances strain localization, and so its inclusion is warranted for a more accurate capture of the bifurcation point. However, a three-invariant constitutive description generally requires a more robust numerical solution algorithm (Borja et al., 2003) in order for the model to be useful in practice.

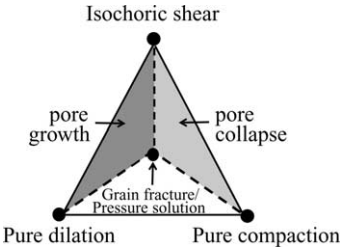

Fig. 12. Idealized diagram showing the parameters that define the three failure modes in porous rock. These are shearing, compaction, dilation and grain fracturing. Compaction and dilation are accommodated by pore collapse/pressure solution or pore enlargement, respectively. Note that the two fields defined by shear/dilation/grain fracture or pressure solution, and shear/compaction/grain fracture or pressure solution (gray shaded) in the diagram are permissible.

8. Mathematical capture of sharp discontinuities

The bifurcation theory for deformation bands signifies the emergence of a 'kink' on the displacement field but does not provide information on the thickness of the band. Classical plasticity theory lacks a characteristic length scale to allow the prediction of the band thickness. Fairly recently, the notion of strong discontinuity has gained much attention in the literature (Borja, 2002 and references therein). 'Strong discontinuity' is an alternative term to denote a jump in the displacement field, and is contrasted with 'weak discontinuity', which is used to describe a jump in the displacement gradient field. In the limiting condition of zero band thickness, a 'kink' characterizing a weak discontinuity becomes a 'slip' characterizing a strong discontinuity.

A criterion for the onset of strong discontinuity developed from theory of distribution has gained acceptance in recent years (see Borja, 2002 and references therein) and takes the form:

$$\det(\tilde{\boldsymbol{A}}) = 0, \qquad \tilde{A}_{ij} = n_k \tilde{c}^{\mathrm{ep}}_{ikjl} n_l, \tag{5}$$

where $\tilde{\boldsymbol{A}}$ (with components $\tilde{A}_{ij}$) is the elastic–perfectly plastic acoustic tensor, and $\tilde{\boldsymbol{c}}^{\mathrm{ep}}$ (with components $\tilde{c}^{\mathrm{ep}}_{ikjl}$) is the tangential elastic–perfectly plastic constitutive tensor. The use of an elastic–perfectly plastic acoustic tensor ensures that the stress rate inside the band remains bounded at the moment of localization (bounded distribution) as the plastic modulus changes in character from its continuum value to a value of order h, where h = band thickness. The criterion for strong discontinuity is contrasted with that for deformation bands in that the former recognizes a vanishing band thickness whereas the latter does not.

9. Discussion and conclusions

In conclusion, we have presented a geological framework that covers the entire spectrum of failure in granular rock. The top categories are sharp discontinuities and narrow tabular bands of localized deformation. The end members for the latter are isochoric shear, pure compaction, and pure dilation (Fig. 12). Field data indicate that although the three end members do occur in nature, mixed-mode localization structures such as compactive shear bands (or compaction bands with shear) and dilatant shear bands (or dilatant bands with shear) are the most common modes of localized failure. Volumetric deformation by means of pore collapse, pressure solution, and grain fracturing is the greatest for compactive shear bands and compaction bands. The micromechanics of failure depend on interplay among grain boundary sliding, pore enlargement or collapse, pressure solution, and grain fracturing, some of which are schematically illustrated in Fig. 13. These mechanisms are controlled by the petrophysical properties of the granular rock and the loading conditions (Vesić and Clough, 1968; Wood, 1990; Mavko et al., 1997).

Among the failure structures considered in this study compaction and dilation bands appear to be most intriguing. More specifically, localization of strain into narrow bands by the growth of pores within the band is in striking contrast to the 'elastic crack' concept based on propagation of individual flaws producing macroscopic planar structures. Also, we described planar shear failure structures formed along pre-existing weak planes in granular rock. In spite of some reports of classic shear fractures/faults in natural environments (Vermilye and Scholz, 1999), there is no unambiguous evidence that shear fractures composed of two planar surfaces initiate, propagate, and develop in pristine granular geomaterials. In this respect, the only structure that is similar in form and concept to the idealized shear fracture/fault is a slip surface (Aydin and Johnson, 1978). This structure, however, has never been observed by itself in an otherwise pristine granular rock (without a zone of shear bands). The appearance of a slip surface always marks the culmination of fault evolution in granular rocks in terms of the fundamental structural components of a fault zone (Aydin and Johnson, 1978; Shipton and Cowie, 2001). Thus,

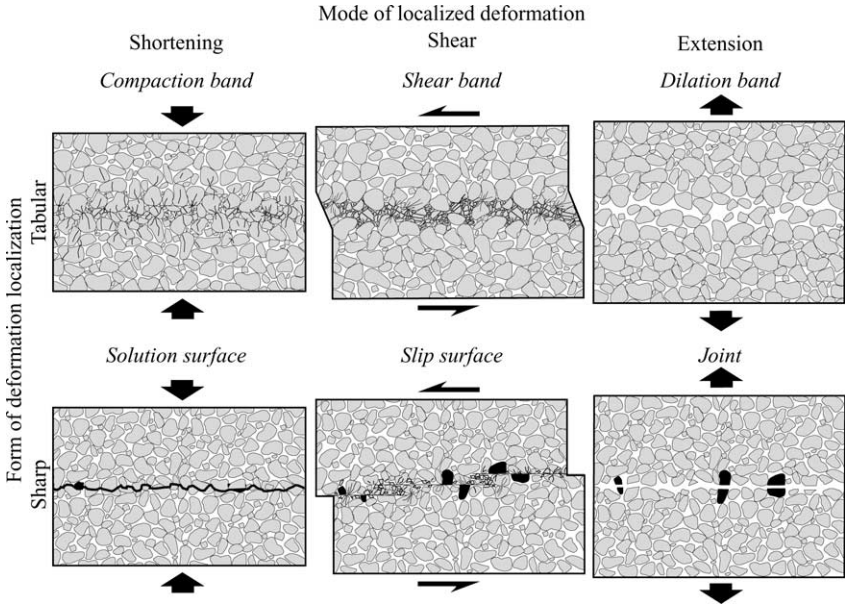

Fig. 13. Schematic illustration of structures resulting from various failure modes in granular rock. Compaction, shearing, and dilation in narrow tabular bands (top row) and sharp discontinuities (bottom row).

the formation of a slip surface differs significantly from that of an idealized shear fracture in terms of its initiation and growth history.

Shear fractures/faults initiated from planar weaknesses differ from idealized shear fractures by their out-of-plane propagation which is crucial for the final geometry and pattern of the system. Faults also develop by overprinting structures (deformation bands, jointing, and subsequent shearing). From the field geology point of view, recognizing and deciphering complex fault zones involving localized tabular deformation structures overprinted by sheared planar failure structures (slip surfaces/sheared joints and solution surfaces) pose challenging future research subjects.

We have also presented a mathematical framework for characterizing the occurrence of tabular bands in geologic materials using classical bifurcation theory and the mathematical theory of plasticity. The formulation is complete in the sense that the end result specifies the type of deformation band expected to form at localization. The characters of the deformation band predicted by the theory depend on the constitutive model, and thus to capture the constitutive response of granular materials more accurately we have presented a class of three-invariant elastoplastic constitutive models. With the aforementioned bifurcation theory, this class of constitutive models provides a mathematical description of the formation of the three extreme failure modes, namely, simple shear, pure compaction, and pure dilation, as well as the combination modes described in the geologic framework. We briefly described a criterion for strong discontinuity and contrasted it with that for deformation bands in that the former recognizes a vanishing band thickness whereas the latter does not.

Acknowledgements

A. Aydin acknowledges financial support through the National Science Foundation grant EAR-02-29862. Partial support was also provided by US Department of Energy grant DE-FG03-94ER14462. R.I. Borja acknowledges support of National Science Foundation grant CMS-02-01317, and US Department of Energy grant DE-FG02-03ER15454. We thank Jennifer Wilson and an anonymous reviewer, David Ferrill, the Editor, for their thoughtful comments.

References

Al-Shaieb, Z., Puckette, J.O., Abdalla, A.A., Tigert, V., Ortoleva, P.J., 1994. The banded character of pressure seals. In: Ortoleva, P.J. (Ed.), Basin Compartments and Seals. AAPG Memoir 61, pp. 351–367.

Antonellini, M.A., Aydin, A., 1994. Effect of faulting on fluid flow in porous sandstones: petrophysical properties. AAPG Bulletin 78, 355–377.

Antonellini, M.A., Aydin, A., Pollard, D.D., 1994a. Microstructure of deformation bands in porous sandstones at Arches National Park, Utah. Journal of Structural Geology 16, 941–959.

Antonellini, M.A., Aydin, A., Pollard, D.D., D'Onfro, D., 1994b. Petrophysical study of faults in sandstones using petrographic image analysis and X-ray computerized tomography. Pure and Applied Geophysics 143, 181–201.

Argon, A.S., 1975. Plastic deformation of glassy polymers. In: Baer, E., Radcliffe, S.V. (Eds.), Polymeric Materials (Relationship Between Structure and Mechanical Behaviour). ASM Monograph. Metals Park, Ohio, pp. 412–486.

Aydin, A., 1978. Small faults formed as deformation bands in sandstone. Pure and Applied Geophysics 116, 913–930.

Aydin, A., Johnson, A.M., 1978. Development of faults as zones of deformation bands and as slip surfaces in sandstone. Pure and Applied Geophysics 116, 931–942.

Aydin, A., Johnson, A.M., 1983. Analysis of faulting in porous sandstones. Journal of Structural Geology 5, 19–31.

Berg, C.A., 1970. Plastic dilation and void interaction. In: Kanninen, M.F., Adler, W.F., Rosenfield, A.R., Jaffee, R.I. (Eds.), Inelastic Behavior of Solids. McGraw-Hill, New York, pp. 171–210.

Berg, C.A., 1972. Ductile fracture by development of surfaces of unstable cavity expansion. Journal of Research of the National Bureau of Standards, Civil Engineering and Instrumentation 76C, 1–2.

Bernabé, Y., Bryer, D.T., Hayes, J.A., 1992. The effect of cement on the strength of granular rocks. Geophysical Research Letters 19, 1511–1514.

Bésuelle, P., 2001. Compacting and dilating shear bands in porous rock: theoretical and experimental conditions. Journal of Geophysical Research 106, 13435–13442.

Bésuelle, P., Rudnicki, J.W., 2004. Localization: shear bands and compaction bands. In: Guéguen, Y., Boutéca, M. (Eds.), Mechanics of Fluid Saturated Rocks. International Geophysics Series 89. Elsevier Academic Press, New York, pp. 219–321.

Bjørlykke, K., Høeg, K., 1997. Effects of burial diagenesis on stresses, compaction and fluid flow in sedimentary basins. Marine and Petroleum Geology 14, 267–276.

Borg, I.Y., Friedman, M., Handin, J.W., Higgs, D.V., 1960. Experimental deformation of Saint Peter sand—a study of cataclastic flow. In: Griggs, D.T., Handin, J.W. (Eds.), Rock Deformation—A Symposium. Geological Society of America Memoir 79, pp. 133–191.

Borja, R.I., 2002. Bifurcation of elastoplastic solids to shear band mode at finite strain. Computer Methods in Applied Mechanics and Engineering 191, 5287–5314.

Borja, R.I., 2003. Algorithm for a class of three-invariant elastoplastic constitutive modes suitable for the analysis of deformation bands in geomaterials. In: Oñate, E., Owen, D.R.J. (Eds.), VII International Conference on Computational Plasticity (COMPLAS 2003), CIMNE, Barcelona, on CD-ROM.

Borja, R.I., 2004. Computational modeling of deformation bands in granular media, II: Numerical simulations. Computer Methods in Applied Mechanics and Engineering 193, 2699–2718.

Borja, R.I., Aydin, A., 2004. Computational modeling of deformation bonds in granular media. I: Geological and mathematical framework. Computer Methods in Applied Mechanics and Engineering 193, 2667–2698.

Borja, R.I., Regueiro, R.A., Lai, T.Y., 2000. FE modeling of strain localization in soft rock. Journal of Geotechnical and Geoenvironmental Engineering 126, 335–343.

Borja, R.I., Sama, K.M., Sanz, P.F., 2003. On the numerical integration of three-invariant elastoplastic constitutive models. Computer Methods in Applied Mechanics and Engineering 192, 1227–1258.

Borradaile, G.J., 1981. Particulate flow of rock and the formation of cleavage. Tectonophysics 72, 305–321.

Brace, W.F., Bombolakis, E.G., 1963. A note on brittle crack growth in compression. Journal of Geophysical Research 68, 3709–3713.

Çakir, M., Aydin, A., 1994. Tectonics and Fracture Characteristics of the Northern Lake Mead, SE Nevada, Proceedings of the Stanford Rock Fracture Project Field Workshop. Stanford University, Stanford.

Cashman, S., Cashman, K., 2000. Cataclasis and deformation-band formation in unconsolidated marine terrace sand, Humboldt County, California. Geology 28, 111–114.

Cooke, M., Mollema, P., Pollard, D.D., Aydin, A., 2000. Interlayer slip and joint localization in the East Kaibab Monocline, Utah: field evidence and results from numerical modeling. In: Cosgrove, J.W., Ameen, M.S. (Eds.), Forced Folds and Fractures. Geological Society, London, Special Publication vol. 169, pp. 23–49.

Cotterell, B., Rice, J.R., 1980. Slightly curved or kinked cracks. International Journal of Fracture 16, 155–169.

Cruikshank, K.M., Aydin, A., 1994. Role of fracture localization in arch formation, Arches National Park, Utah. Geological Society of America Bulletin 106, 879–891.

Cruikshank, K.M., Zhao, G., Johnson, A.M., 1991. Analysis of minor fractures associated with joints and faulted joints. Journal of Structural Geology 13, 865–886.

Curran, J.H., Carroll, M.M., 1979. Shear enhancement of void compaction. Journal of Geophysical Research 84, 1105–1112.

Davatzes, N.C., Aydin, A., 2003. Overprinting faulting mechanisms in sandstone. Journal of Structural Geology 25, 1795–1813.

Davatzes, N.C., Aydin, A., 2004. Overprinting faulting mechanisms in high porosity sandstones of SE Utah. Journal of Structural Geology 25, 1795–1813.

Davatzes, N.C., Aydin, A., Eichhubl, P., 2003. Overprinting faulting mechanisms during the development of multiple fault sets in sandstone, Chimney Rock fault array, Utah, USA. Tectonophysics 363, 1–18.

Davis, G.H., 1999. Structural geology of the Colorado Plateau region of southern Utah. Geological Society of America Special Paper, 342.

DiGiovanni, A.A., Fredrich, J.T., Holcomb, D.J., Olsson, W.A., in press. Microscale damage evolution in compacting sandstone. In: Couples, G.D., Lewis, H., Meredith, P. (Eds.), Relationships Between Fracture Damage and Localisation. Geological Society, London, Special Publications.

Drucker, D.C., Prager, W., 1952. Soil mechanics and plastic analysis or limit design. Quarterly Applied Mathematics 10, 157–165.

Du Bernard, X., Eichhubl, P., Aydin, A., 2002. Dilation bands, a new form of localized failure in granular media. Geophysical Research Letters 29 (24), 2176 doi: 1029/2002GLO15966.

Dunn, D.E., Lafountain, L.J., Jackson, R.E., 1973. Porosity dependence and mechanism of brittle faulting in sandstone. Journal of Geophysical Research 78, 2303–2317.

Dvorkin, J., Nur, A., 1996. Elasticity of high-porosity sandstones: theory for two North Sea data sets. Geophysics 61, 1363–1370.

Engelder, T., 1974. Cataclasis and the generation of fault gouge. Geological Society of America Bulletin 85, 1515–1522.

Engelder, T., 1987. Joints and shear fractures in rock. In: Atkinson, B.K. (Ed.), Fracture Mechanics of Rock. Academic Press, London, pp. 27–69.

Fletcher, R.C., Pollard, D.D., 1981. Anticrack model for pressure solution surfaces. Geology 9, 419–424.

Fossen, H., Hesthammer, J., 1997. Geometric analysis and scaling relations of deformation bands in porous sandstone. Journal of Structural Geology 19, 1479–1493.

Friedman, M., Logan, J.M., 1973. Luders' bands in experimentally deformed sandstone and limestone. Geological Society of America Bulletin 84, 1465–1476.

Gallagher, J.J., 1987. Fractography of sand grains broken by uniaxial compression. In: Marshall, J.R. (Ed.), Classic Particles. Van Nostrand Reinhold, New York, pp. 189–228.

Groshong Jr., R.H., 1988. Low-temperature deformation mechanisms and their interpretation. Geological Society of America Bulletin 100, 1329–1360.

Haimson, B.C., 2001. Fracture-like borehole breakouts in high-porosity sandstone: are they caused by compaction bands? Physics and Chemistry of the Earth 26, 15–20.

Hill, R., 1958. A general theory of uniqueness and stability in elastic–plastic solids. Journal of the Mechanics and Physics of Solids 6, 236–249.

Hill, R.E., 1989. Analysis of deformation bands in the Aztec Sandstone, Valley of Fire, Nevada. MS Thesis, Geosciences Department, University of Nevada, Las Vegas.

Hubbert, M.K., Rubey, W.W., 1959. Mechanics of fluid-filled porous solids and its application to overthrust faulting, [Part] 1 of role of fluid pressure in mechanics of overthrust faulting. Geological Society of America Bulletin 70, 115–166.

Issen, K.A., Rudnicki, J.W., 2000. Conditions for compaction bands in porous rock. Journal of Geophysical Research 105, 21529–21536.

Jaeger, J.C., Cook, N.G.W., 1979. Fundamentals of Rock Mechanics, 3rd ed. Chapman & Hall, New York.

Lade, P.V., Duncan, J.M., 1975. Elastoplastic stress-strain theory for cohesionless soil. Journal of Geotechnical Engineering Division, ASCE 101, 1037–1053.

Mair, K., Main, I., Elphick, S., 2000. Sequential growth of deformation bands in the laboratory. Journal of Structural Geology 22, 25–42.

Mandel, J., 1966. Conditions de stabilité et postulat de Drucker, Proceedings IUTAM Symposium on Rheology and Soil Mechanics. Springer, Berlin pp. 58–68.

Matsuoka, H., Nakai, T., 1974. Stress-deformation and strength characteristics of soil under three different principal stresses. Proceedings of the Japanese Society of Civil Engineers 232, 59–70.

Mavko, G., Mukerji, T., Dvorkin, J., 1997. The Rock Physics Handbook. Tools for Seismic Analysis of Porous Media. Cambridge University Press, Cambridge.

Menéndez, B., Zhu, W., Wong, T.-F., 1996. Micromechanics of brittle faulting and cataclastic flow in Berea sandstone. Journal of Structural Geology 18, 1–16.

Mollema, P.N., Antonellini, M.A., 1996. Compaction bands: a structural analog for anti-mode I cracks in aeolian sandstone. Tectonophysics 267, 209–228.

Myers, R.D., 1999. Structure and hydraulic properties of brittle faults in sandstone. PhD Thesis, Stanford University, Stanford.

Myers, R.D., Aydin, A., 2004. The evolution of faults formed by shearing across joint zones in sandstone. Journal of Structural Geology 26, 947–966.

Olsson, W.A., 1999. Theoretical and experimental investigation of compaction bands in porous rock. Journal of Geophysical Research 104, 7219–7228.

Olsson, W.A., 2000. Origin of Lüders' bands in deformed rock. Journal of Geophysical Research 105, 5931–5938.

Pittman, E.D., 1981. Effect of fault-related granulation on porosity and permeability of quartz sandstones, Simpson Group (Ordovician), Oklahoma. American Association of Petroleum Geologists Bulletin 65, 2381–2387.

Pollard, D.D., Aydin, A., 1988. Progress in understanding jointing over the past one hundred years. Geological Society of America Bulletin 100, 1181–1204.

Pollard, D.D., Segall, P., 1987. Theoretical displacements and stresses near fractures in rock: with applications to faults, joints, veins, dikes, and solution surfaces. In: Atkinson, B.K. (Ed.), Fracture Mechanics of Rock. Academic Press, London, pp. 277–349.

Rawling, G.C., Goodwin, L.B., 2003. Cataclastic and particulate flow in faulted, poorly lithified sediments. Journal of Structural Geology 25, 317–331.

Renard, F., Brosse, É., Gratier, J.P., 2000. The different processes involved in the mechanism of pressure solution in quartz-rich rocks and their interactions. In: Worden, R.H., Morad, S. (Eds.), Quartz Cementation in Sandstones Special Publication Number 29 of the International Association of Sedimentologists. Blackwell, London, pp. 67–78.

Rudnicki, J.W., 2002. Conditions for compaction and shear bands in a transversely isotropic material. International Journal of Solids and Structures 39, 3741–3756.

Rudnicki, J.W., Olsson, W.A., Rice, J.R., 1975. Conditions for the localization of deformation in pressure-sensitive dilatant materials. Journal of the Mechanics and Physics of Solids 23, 371–394.

Segall, P., Pollard, D.D., 1983. Nucleation and growth of strike-slip faults in granite. Journal of Geophysical Research 88, 555–568.

Shah, K.R., Wong, T.-F., 1997. Fracturing at contact surfaces subject to normal and tangential loads. International Journal of Rock Mechanics and Mining Sciences 34, 727–739.

Shipton, Z.K., Cowie, P.A., 2001. Damage zone and slip-surface evolution over μm to km scales in high-porosity Navajo sandstone, Utah. Journal of Structural Geology 23, 1825–1844.

Sternlof, K., Pollard, D.D., 2001. Deformation bands as linear elastic fractures: progress in theory and observation. Eos Transactions American Geophysical Union 82 (47), F1222.

Sternlof, K., Pollard, D., 2002. Numerical modelling of compactive deformation bands as granular anti-cracks. Eos Transactions American Geophysical Union 87 (47), F1347.

Thomas, T.Y., 1961. Plastic Flow and Fracture of Solids. Academic Press, New York.

Vermilye, J.M., Scholz, C.H., 1999. Fault propagation and segmentation; insight from the microstructural examination of a small fault. Journal of Structural Geology 21, 1623–1636.

Vesić, A.S., Clough, G.W., 1968. Behaviour of granular materials under high stresses. Journal of the Soil Mechanics and Foundation Division Proceedings of the American Society of Civil Engineers 94, 661–688.

Wilson, J.E., Goodwin, L.B., Lewis, C.J., 2003. Deformation bands in nonwelded ignimbrites: petrophysical controls on fault-zone deformation and evidence of preferential fluid flow. Geology 31, 837–840.

Wong, T.-F., David, C., Zhu, W.L., 1997. The transition from brittle faulting to cataclastic flow in porous sandstones: mechanical deformation. Journal of Geophysical Research 102, 3009–3025.

Wong, T.-F., Baud, P., Klein, E., 2001. Localized failure modes in a compactant porous rock. Geophysical Research Letters 28, 2521–2524.

Wong, T.-F., David, C., Menéndez, B., 2004. Mechanical compaction. In: Guéguen, Y., Boutéca, M. (Eds.), Mechanics of Fluid Saturated Rocks. International Geophysics Series 89. Elsevier Academic Press, New York, pp. 55–114.

Wood, D.M., 1990. Soil Behavior and Critical State Soil Mechanics. Cambridge University Press, Cambridge.

Zhang, J., Wong, T-F., Davis, D.M., 1990. Micromechanics of pressure-induced grain crushing in porous rocks. Journal of Geophysical Research 95, 341–352.

Zhao, G., Johnson, A.M., 1992. Sequence of deformation recorded in joints and faults, Arches National Park, Utah. Journal of Structural Geology 14, 225–236.